Damage detecting roller device based on electromechanical impedance technique for debonding detection in glass fiber epoxy composite structures

Yi-Seul Kim and Wongi S. Na*

Department of Civil Engineering, Seoul National University of Science & Technology, 232 Gongneung-ro, Nowon-gu, Seoul, Republic of Korea

* Corresponding Author: wongi@seoultech.ac.kr;.

ABSTRACT

Maintaining structural safety for the public is one of the most utmost importance to avoid catastrophic events involving human casualty. For this reason, vast amount of research is being conducted around the globe to create an efficient system to detect structure damage. In this study, a local damage detection method known as the electromechanical impedance method is improved with the new concept introduced in this study. The idea allows one to detect debonding of composite structures at a reduced cost. Since the electromechanical impedance requires one to permanently attach the piezoelectric (PZT) transducer onto the target structure, a moving device was made which creates temporarily contact with the target structure to investigate the possibility of replacing hundreds of PZT transducers into a single device. The experiment involves using two different glass fiber epoxy composite plates with different thicknesses to evaluate the performance of the roller PZT device. The findings from the experiments show possibility of detecting debonding of composite plate using the proposed idea.

Keywords: Dynamic analysis; riser; Thermoplastic; Offshore jacket; Wave.

INTRODUCTION

In general, countries that have experienced rapid industrialization and economic growth have resulted in constructing many infrastructures. At that time, the priority was to build infrastructures as fast as possible where one could say that the future maintenance part of the construction was a less important factor. With time, buildings experience damage and deterioration where maintenance has become one of the most important tasks for current architectural and civil engineers. As the goal of an efficient maintenance system is to remove harmful factors in advance to maintain the function of the structure, repair damaged parts and to extend the life of the structure, it is important for one to locate any existence of damage at a low cost. Up to date, various studies have been conducted in the past using piezoelectric(PZT) transducers to identify damage in structures. Due to the fact that PZT transducers are suitable for use in structures for their advantages such as low cost and small in size, research is being carried out around the world.

In this study, a local damage detection method known as the electromechanical impedance(EMI) technique is used in conjunction with a new idea to possibly allow the EMI technique to be made into an automatic monitoring system in the future. Here, debonding of glass fiber epoxy composite plates were investigated with the proposed idea where various studies have shown that the EMI technique can detect damage areas in composites. Selva et al presented a study using the EMI technique for in situ damage detection and localization in carbon fiber reinforced plates(CFRPs) (Selva et al., 2013). Here, numerical simulations were also conducted on hundred damage scenarios where results show promising outcome for detecting damage in a laminated composite plate. Zhu et al performed experiments on a repaired composite structure with a 3x3 sensor array where EMI technique was used to monitor debonding between repaired patch and substrate (Zhu et al., 2019). Cherrier et al investigated on generating a damage

localization map based on both indicators computed from EMI spectrums and inverse distance weighting interpolation on both 1-D and 2-D composite structures (Cherrier et al., 2013). Bois and Hochard used EMI technique to detect delamination of laminated composites where the final goal of the study is to predict the damage in the composite structure under static and fatigue loading (Bois & Hochard, 2004). Malinowski et al focused on the glass fiber reinforced polymer(GFRP) beam and plate where both impact and delamination damage was introduced. Also, the authors developed a data processing tool based on principal component analysis to show its advantage over traditional damage index method (Malinowski et al., 2021). Additional studies can be found in (Song et al., 2015, Oliveira & Inman, 2015, Yocum et al., 2003, Wang et al., 2021, Na, 2019, Wandowski et al., 2021) where the studies show how promising that the EMI technique is against detecting damage in composite structure. However, most of the studies require one to permanently attach the PZT transducer onto the target structure for damage detection. This conventional way of attaching the PZT transducer show promising results but at a high cost if one were to monitor a large area or structure. Due to the relatively low sensing range, vast amount of PZT transducers would be required to cover the structure. For this reason, a new concept of EMI technique was proposed that can be rolled onto the surface of a composite structure for detecting delamination. Such idea can significantly reduce the cost of the EMI technique to monitor a structure as only one PZT transducer is required to cover the whole area or the structure.

EMI METHOD AND DATA ANALYSIS

EMI Technique

In this study, the electromechanical impedance (EMI) technique is used to predict the change in the mechanical impedance of the structure by observing the change in the electrical impedance of the PZT transducer. Liang et al. expressed the relationship between the reciprocal of the electrical impedance of the PZT transducer, the electrical admittance, $Y(\omega)$, and the mechanical impedance of the PZT transducer, $Z_a(\omega)$ and the structure, $Z_s(\omega)$ in a one-dimensional equation (Liang et al., 1996). This equation proves that one can acknowledge any change in the structure by measuring the electrical impedance of the PZT transducer attached to the structure.

$$Y(\omega) = i\omega a\left(\varepsilon_{33}^T(1 - i\delta) - \frac{Z_s(\omega)}{Z_s(\omega)+Z_a(\omega)}d_{3X}^2\overline{Y}_{XX}^E\right) \tag{1}$$

EMI technique can be conducted using the AD5933 evaluation board which can measure impedance up to 100 kHz with over 500 data points. Although that this device has the lowest performance when compared to the rest of the devices, it is the smallest and lightest device which can easily be carried around. This is an important factor when locating damage in real field. Shown in Figure 1, the AD5933 evaluation board is connected to a computer and a PZT transducer that is attached to a roller structure which will be explained in details in a later section. The PZT transducer model PSI-5A4E was used where the test specimen was made by attaching two glass fiber reinforced plastic (FRP) plates cut into 210 mm*210 mm with different thicknesses. Regarding the attachment of the FRP plates, the plate is divided into 9 areas (70 mm x 70 mm for each area) where only Area 2, 4, 6 and 8 are attached using an epoxy adhesive. The reason for this is to evaluate the performance of the roller PZT device introduced in this study to detect areas that are not attached as debonding is one of the serious problems when dealing with composite structures. All tests were performed at 24 °C (± 0.1 °C) to minimize the fluctuations in impedance signatures subjected to temperature differences.
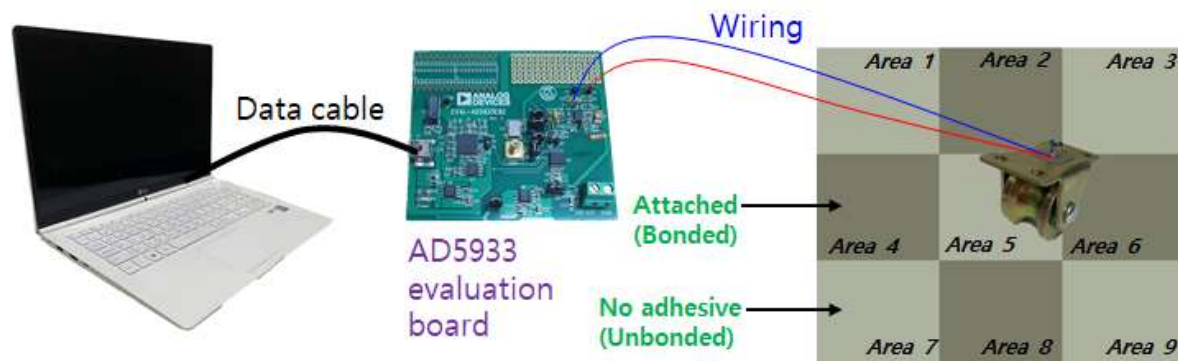

Figure 1. Experimental setup for the FRP plate

After acquiring impedance signatures, the next step is to determine the severity of damage (for this study, attached or no adhesive cases) by analyzing the data. In general, impedance signatures will change greater with more damage. Thus, to quantify this change into a single number, a statistical method known as RMSD (root mean square deviation) is used where it is expressed in equation 2. RMSD has been used widely for studies related to EMI technique by various authors (Wang et al., 2018). The variables N, Z_i^o and Z_i represent the number of signatures, signatures before and after damage, respectively.

$$RMSD = \sqrt{\sum_N[Re(Z_i) - Re(Z_i^o)]^2 / \sum_N[Re(Z_i^o)]^2} \qquad (2)$$
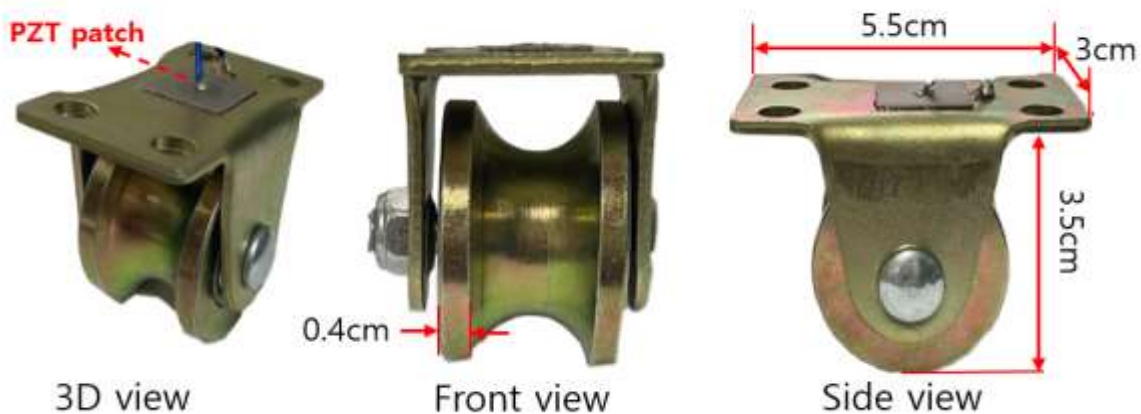
ROLLER EMI DEVICE CREATION

Figure 2. Roller PZT device concept

When conducting the EMI technique, a PZT transducer is directly attached to the target structure permanently. Such setup has the advantage of create an online structural health monitoring system to manage the structures. However, civil infrastructures can be large in size and it would be very costly to cover the building with PZT transducers and devices to measure them. For this reason, the authors have proposed a concept of using a roller device where a 15 mm x 15 mm PZT transducer was permanently attached to the top surface of the roller device as shown in Figure 2. The advantage of this concept is that the wheel allows the device to move freely on a structure such as the FRP plate shown in Figure 1. The contact between the wheel and the FRP plate is made where this study investigates the possibility of using such concept for detecting debonding areas (areas with no adhesive between the two plates). The main part of the experiment explained from next section involves manually rolling the device onto each of 9 areas to investigate the difference in signatures between the bonded and unbonded areas. Such idea would be one of the key technologies for the rising industry of smart construction where the next step for this research would be to create a robot with wheels to automatically inspect a structure to ensure safety for the public.

EXPERIMENT SETUP AND RESULTS

The test setup shown in Figure 1 was used to evaluate the performance of the proposed idea where two test specimens were made. The first test specimen was made by attaching two FRP plates of size 210 mm x 210 mm with 0.2 mm thickness where this will be referred to as 0.2_FRP for the remainder of the study. The second specimen was made by attaching two FRP plates of the same size (210 mm x 210 mm) but with two different thicknesses of 0.2 mm and 0.6 mm. This will be referred to as 0.6_FRP for the remainder of the study. For both 0.2_FRP and 0.6_FRP, the frequency range of 43.5 ~ 45 kHz was used to measure both real and imaginary part of impedance. The roller would be placed anywhere from Area 1 to Area 9 of the FRP plate where the AD5933 evaluation board is then used to acquire the necessary data.

The first set of tests was conducted on 0.2_FRP where 10 impedance signatures were measured on bonded areas (no damage case). Thus, any areas of Area 2, Area 4, Area 6 and Area 8 were measured by simply placing the roller PZT device on top of the FRP plate. After the first 10 impedance measurements acquired from the bonded areas, another 10 impedance signatures were measures on unbonded areas (damaged case) to compare the signature

differences between bonded and unbonded areas. The unbonded areas are Area 1, Area 3, Area 5, Area 7 and Area 9 where both real and imaginary part of impedance were measured for all measurements.

Then, the second set of tests was conducted on 0.6_FRP where 10 impedance signatures were measured on bonded areas. Thus, any areas of Area 2, Area 4, Area 6 and Area 8 were measured by simply placing the roller PZT device on top of the FRP plate. After the first 10 impedance measurements, another 10 impedance signatures were measures on unbonded areas. The unbonded areas are Area 1, Area 3, Area 5, Area 7 and Area 9. The results for the all tests are explained in the next section.

RESULTS AND DISCUSSION

Experimental results on 0.2_FRP

Figure 3 shows impedance signatures conducted using 0.2_FRP test specimen where Figure 3 (a) and (b) are the real parts of the impedance signature measured 10 times from the bonded and unbonded area, respectively. Here, the impedance signatures show variations where the peak is at its highest between 44.1 kHz and 44.2 kHz for Figure 3(a). Although that all the impedance signatures were measured on bonded areas, the signature difference can be easily seen. There is up and down movement of the impedance peak with different measurements as shown in the figure. To quantify how severe the differences in signatures is, all combinations

of 2 impedance signatures out of 10 signatures were used to calculate the RMSD values ($^{10}C_2 = 45$ combinations). From 45 RMSD calculations, the largest RMSD value was 10.82%. Next looking at Figure 3(b), although that the up and down movement of the impedance peak at around 44.2 kHz is smaller compared to Figure 3(a), left and right shift movements for the signature throughout the entire frequency range can be seen. Such difference can lead to a large RMSD value when comparing two signatures. As expected, the largest RMSD value of 20.50% was calculated when comparing two signatures from the rest of the impedance signatures. Since it is difficult to visually identify which set of impedance signatures belong to unbonded or bonded areas, the signatures were averaged where this is shown in Figure 3(c). Here it is clear that there is a difference between the two different cases. The averaged impedance signature for the unbonded case has higher impedance peak compared to the averaged impedance signature for the bonded case. When the RMSD value is calculated using the two averaged signatures, 13.90% is obtained which is larger when compared to 10.82% obtained from using Figure 3(a) and smaller compared to 20.50% obtained from Figure 3(b). Therefore, it would not be suitable for one to identify presence of damage with single measurement. An acceptable way would to be measure multiple times to average the signature for comparison to increase the accuracy of the outcome. For an example, if one were to identify which of Area 1 and Area 2 is damaged, 10 random measurements using the roller PZT device should be used to average the obtained signature. Then the impedance signature with the higher peak would indicate that the area is damaged. For this case, it would be Area 1. Next observing at the imaginary part of the impedance for the same test on Figure 3(d) and 3(e), the behavior of how impedance signatures change is quite similar to the real part of impedance explained above. Again, up and down movements are mainly observed for Figure 3(d) where left and right movements are mainly observed for Figure 3(e). Regarding the highest RMSD values between two impedance signatures that has the largest difference, the values were 4.70 % and 9.54 % for Figure 3(d) and Figure 3(e), respectively. Figure 3(f) shows the averaged impedance signatures from the previous two figures where clear difference is seen between the two different cases. Here, although that the unbonded case signature has lower peak value compared to the bonded case, the size of the peak is larger(both impedance signatures start at around 6500 ohms and the unbonded case decreases down to 1000 ohms), meaning that more severe vibration was experienced with the unbonded case. When the RMSD value was calculated for this figure, 6.58% was acquired.
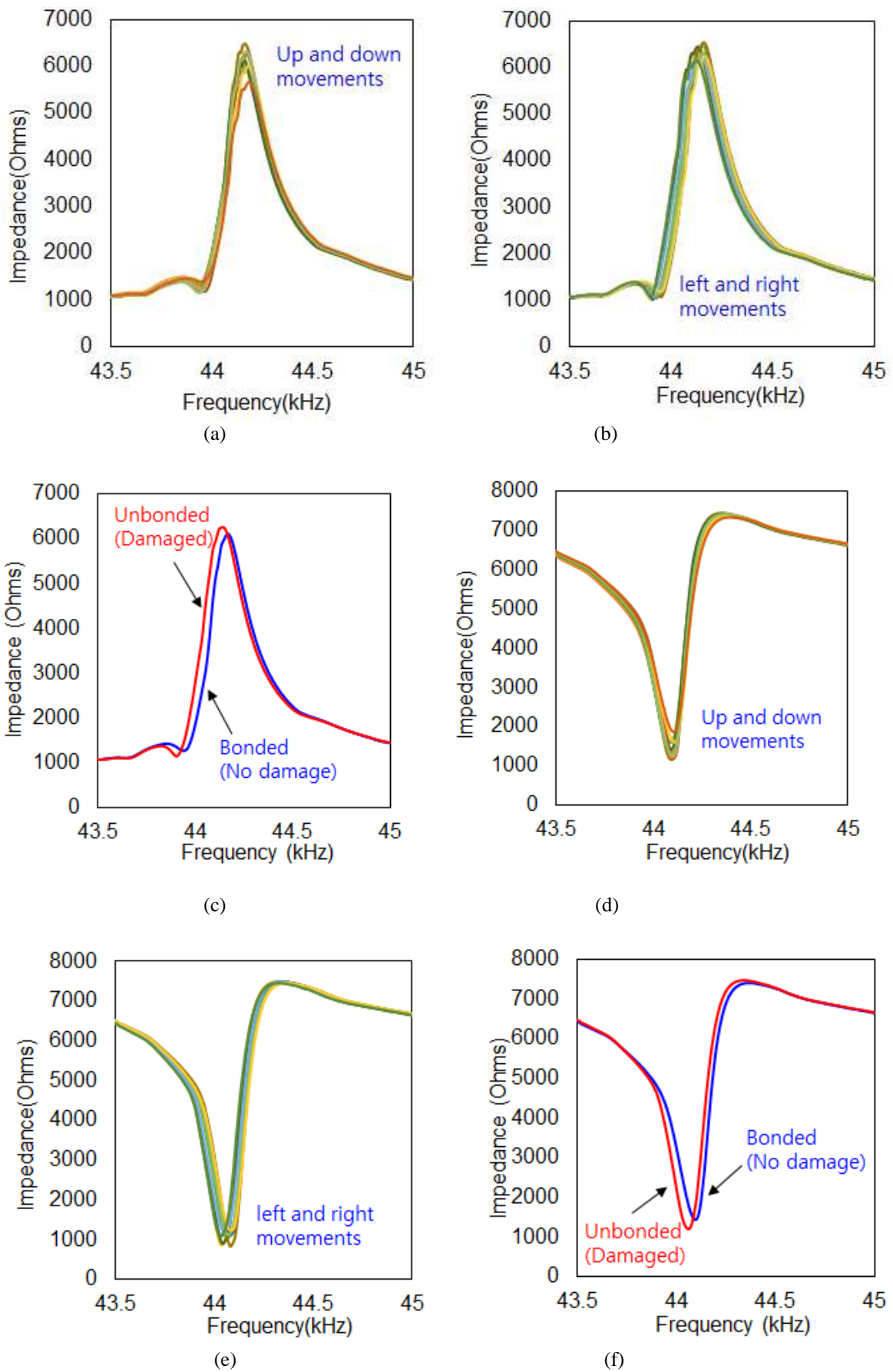
Figure 3 Real part of Impedance signatures for 0.2_FRP on (a) unbonded area, (b) bonded area, (c) averaged signature. Im aginary part for (d) unbonded area, (e) bonded area, (f) averaged signature.

Experimental results on 0.6_FRP

In Figure 3, impedance signatures were plotted in a 2-D format to investigate signature variations. Although that the difference was clearly observed using 2-D plots, creating a 3-D graph would enhance the visibility of how the impedance signatures change. Thus, in this section, 10 real part of impedance signatures from bonded and unbonded areas have been acquired for 0.6_FRP and is shown in Figure 4(a). The two different cases (bonded and unbonded areas) have been labelled in the figure where variations between signatures can be seen. One observation is that the signatures from unbonded area have higher peaks compared to bonded area where this can be identified by the amount of green areas locate at the top of the peaks. The largest RMSD values for both cases when comparing two impedance signatures were 9.12 % and 9.70 % for bonded and unbonded cases respectively. The averaged signatures for both cases are shown in Figure 4(b) where the signature for the unbonded case has higher peak compared to bonded case as expected. Here, the RMSD value of 6.03 % was calculated which is smaller than the previous values of 9.12 % and 9.70 %. Thus, once again this experimentally proves that using a single measurement for identifying the presence of damage can be misleading and multiple measurements should be carried out to increase the accuracy of the outcome. Next Figure 4(c) shows the averaged impedance signatures for the imaginary part of impedance where the amplitude size of the impedance signature for the unbonded case is larger than bonded case. Here, 10 impedance signatures for the bonded case and unbonded case was averaged to be plotted into Figure 4(c) where the largest RMSD value within the bonded case and unbonded case were 7.01 % and 5.10 %, respectively. These values are larger than the

RMSD value obtained for the averaged lines of 2.43 % once again, experimentally proving that multiple measurements should be taken ensure correct outcome when identifying damage.
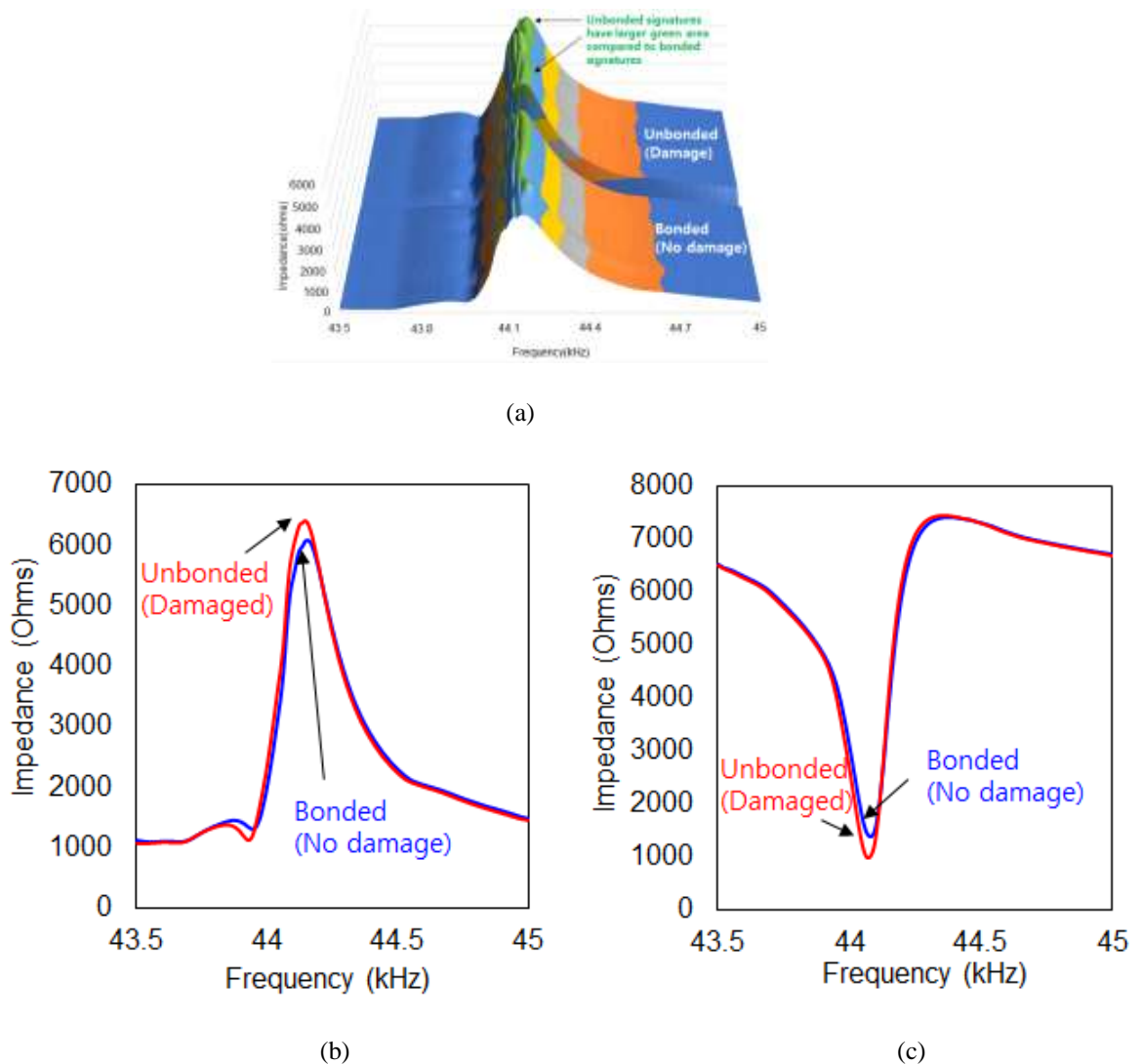

(a)

(b)

(c)

Figure 4 (a) 3-D plot for experiment on 0.6_FRP, averaged signatures for (b) real part of impedance, (c)

imaginary part of imp edance

Comparison of averaged signatures for 0.2_FRP and 0.6_FRP

From both test specimens, one can say that by measuring the impedance signature multiple times (for this study, 10 measurements for either bonded or unbonded area) and averaging the data can allow one to distinguish between damaged case from an undamaged case. From both experiments, it was found that with real part of impedance signature, the unbonded(damaged) area has higher peak amplitude compared to the bonded area as shown in Figure 3(c) and Figure 4(b) where this fact can be used to identify damage. However, the RMSD value for Figure 3(c) of 13.90 % is more than twice the RMSD value from Figure 4(b) of 6.03 %. Thus, this experimentally proves that the proposed idea performs better subjected to thinner FRP plate. Similar outcome is observed for the imaginary part of the impedance of 6.58 % for Figure 3(f) and 2.43 % for Figure 4(b) where the thinner FRP plate has higher value compared to 0.6_FRP. One can conclude by setting the threshold value of 6 % when using the real part of impedance for distinguishing between a damages case from an undamaged case by averaging 10 impedance signatures as both 0.2_FRP and 0.6_FRP shows a value of 13.90 % and 6.58 %.

CONCLUSIONS

In this study, a new concept of roller PZT device was introduced for efficient damage monitoring of composite structures subjected to damage.

For the actual experiment, two test specimens labeled 0.2_FRP and 0.6_FRP were made. 0.2_FRP was made by partially adhering two glass fiber epoxy plates of size 210 mm x 210 mm with 0.2 mm thickness. 0.2_FRP was made by partially adhering the two composite plates of the same size but with two different thicknesses of 0.2 mm and 0.6 mm where one of the studies was to investigate how the proposed idea of roller PZT device work on different thickness structures. Then the roller PZT device was placed on top of the test specimen where 10 impedance signatures were measured on unbonded(damaged) and bonded(no damage) areas to acquire total of 20 signatures each for 0.2_FRP and 0.6_FRP in the frequency range of 43.5 kHz ~ 45 kHz. Both the real and imaginary parts of impedance were measured to investigate how the signatures vary.

First with the 0.2_FRP experiment result, large variations in the signatures were noticed with 10 consecutive measurements where the largest RMSD values (signature difference) were 10.82 %, and 20.50 % for bonded and unbonded areas, respectively. These numbers can be said to be large and such values can result in fault alarms. This problem was solved by averaging each of 10 impedance signatures into a single signature for comparison. The RMSD value of 13.90 % was obtained with the unbonded area having higher impedance peak. This experimentally showed that instead of using single measurement, multiple measurements should be taken to identify damage. Lastly with the 0.6_FRP experiment, the largest RMSD values were 9.12 % and 9.70 % for bonded and unbonded cases respectively. When the signatures were averaged for comparison, 6.03 % was acquired once again proving that using multiple measurements is important for identifying damage. Also, with the imaginary part, the, the RMSD values of 2.43 % was obtained when each of 10 impedance signatures were averaged for RMSD calculation. Overall, regardless of the different thickness of the composite plate, over 6 % RMSD values were calculated with the averaged signatures when using the real part of impedance. Thus, a threshold value of 6 % can be used to detect debonding of glass epoxy composite plate of thickness up to 0.6 mm as experimentally shown in this study.

ACKNOWLEDGEMENT

REFERENCES

Selva, P., Cherrier, O., Budinger, V., Lachaud, F. & Morlier, J. 2013. Smart monitoring of aeronautical composites plates based on electromechanical impedance measurements and artificial neural networks. Engineering Structures 56: 794-804.

Zhu, J., Wang, Y. & Qing, X. 2019. A real-time electromechanical impedance-based active monitoring for composite patch bonded repair structure. Composite Structures, 212: 513-23.

Cherrier, O., Selva, P., Pommier-Budinger, V., Lachaud, F. & Morlier, J. 2013. Damage localization map using

electromechanical impedance spectrums and inverse distance weighting interpolation: Experimental validation on thin composite structures. Structural Health Monitoring, 12(4): 311-24.

Bois, C. & Hochard, C. 2004. Monitoring of laminated composites delamination based on electro-mechanical impedance measurement. Journal of Intelligent Material Systems and Structures 15(1): 59-67.

Malinowski, P. H., Wandowski, T. & Singh, S. K. 2021. Employing principal component analysis for assessment of damage in GFRP composites using electromechanical impedance.

Composite Structures 266: 113820.

Song, J., Nguyen, D. L., Manathamsombat, C. & Kim, D. J. 2015. Effect of fiber volume content on electromechanical behavior of strain-hardening steel-fiber-reinforced cementitious composites. Journal of Composite Materials 49(29): 3621-34.

de Oliveira, M. A. & Inman, D. J. 2015. PCA-based method for damage detection exploring electromechanical impedance in a composite beam. Structural Health Monitoring 2015: 2015

Yocum, M., Abramovich, H., Grunwald, A. & Mall, S. 2003. Fully reversed electromechanical fatigue behavior of composite laminate with embedded piezoelectric actuator/sensor. Smart materials and structures 12(4): 556.

Wang, J., Li, W., Lan, C. & Wei, P. 2021. Effective determination of Young's modulus and Poisson's ratio of metal using piezoelectric ring and electromechanical impedance technique: A proof-of-concept study. Sensors and Actuators A: Physical 319:112561.

Na, W. S. 2019. History data free piezoelectric based non-destructive testing technique for debonding detection of composite structures. Composite Structures 226:111225.

Wandowski, T., Malinowski, P. H. & Ostachowicz, W. M. 2021. Improving the EMI-based damage detection in composites by calibration of AD5933 chip. Measurement 171: 108806.

Moll, J., Schmidt, M., Käsgen, J., Mehldau, J., Bücker, M. & Haupt, F. 2020. Detection of Pin Failure in Carbon Fiber Composites Using the Electro-Mechanical Impedance Method. Sensors 20(13): 3732.

Liang, C., Sun, F. & Rogers, C. A. (1996). Electro-mechanical impedance modeling of active material systems. Smart Materials and Structures 5(2): 171.

Wang, Z., Chen, D., Zheng, L., Huo, L. & Song, G. 2018. Influence of axial load on electromechanical impedance (emi) of embedded piezoceramic transducers in steel fiber concrete. Sensors 18(6): 1782.